DYNAMIC BEHAVIOR OF LNG INGROUND TANK

M. Hoshiya (I)
Y. Yamaguchi (II)
M. Tsujita (III)
K. Wakita (IV)
Presenting Author: M. Tsujita

SUMMARY

This paper investigated experimentally as well as analytically the effects of the tank depth and the rigidity of the joint between base slab and wall on dynamic characteristics of LNG cylindrical inground tank in soft alluvial soil layers of the shear wave velocity of 100m/s to 200m/s. The results obtained were checked and discussed in comparison with current aseismic design methods.

INTRODUCTION

LNG inground storage tanks were first built in around 1960 in Japan and they are relatively new type of structure built in the ground. This specific type of tank has experienced no severe shocks from major earthquake to date and has been closely observed up to now on the occasion of each earthquake (Ref.1). In addition, many tests have also been conducted on a single tank and/or tanks in groups(Ref.2) of the same type (Ref.3) together with research work on sloshing phenomenon (Ref.4).

However, so far no research work has been carried out on the embedded depth and rigidity of the joint between base slab and wall. We therefore commenced studies in order to clarify a possible impact of the embedded depth and the rigidity of the joint between base slab and wall to find out to what an extent its aseismicity can be ensured.

TESTS AND NUMERICAL ANALYSIS

Assumption was made on the soil ground having two layers of 60m thick alluvium (Vs = 130m/s and 210m/s) and on two tanks (60,000kl and 90,000kl) each having diameter of 60m, 3m thick sidewall, 7m thick base concrete and embedded respectively in the depth of 27 and 47m.

A law of similarity was set according to the dimensional analysis method. As the testing materials, plasti-sol (polyvinyl chloride + dioctyl phthalate) for ground model and urethane with hardness of 90° for tank models were used. Also in the neighborhood of a ground model, a visco-boundary layer (oil + urethane mat) was made. Fig. 1 shows an external shape of the test model and Table 1 physical constants.

(I) Professor of Civil Engineering, Musashi Inst. of Technology, Tokyo, Japan
(II) Eng. Manager, Tech. Laboratory, Hazama-Gumi, Ltd., Tokyo, Japan
(III) Senior Research Engineer, "
(IV) Research Engineer, "

Loading acceleration was set as a harmonic excititon with a vibrating table as a base. The amplitude of a vibrating table was set as 1mm on an average while the frequency ranges as 0.5 - 25Hz. Items to be measured were acceleration, displacement, phase angle and dynamic strain. To measure the first 3 items, 13 accelerometers were installed on both ground and tank wall and, in addition, 18 strainmeters on the tank wall.

To seek a possible impact arising from the embedded depth of the tank, tests were conducted by varying the embedded depth of the tank to 9cm and 14cm. Further, to prove the impact arising from the rigidity of the joint between base slab and wall, tests were conducted on the tanks a) without base slab (cylinder model) and b) with base slab rigidly connected to the side wall of the tank. The former was based on the assumption that the tank was built incorporating a free connection of base slab to the side wall (a combined crossing construction) or by a pin connection of the base slab to the side wall (a combined construction by PC steel bars) and both consist only of a side wall structure against the external force of earthquake, while the latter was based on the assumption that the base concrete was rigidly and completely connected to the side wall.

All tests were conducted on the assumption that there was no liquid contained in the tank, but, in the final stage, tests were conducted on the assumption that the tank was full of liquid. To simulate this load plates corresponding to the weight of full liquid in the tank were added to the side wall of the tank. The other one was also conducted on the natural soil ground as a model.

Analysis was made on axi-symmetric finite element model and to further confirm ovaling phenomenon, analysis was also made on a three dimensional finite element model for the two different types of a 14cm deep model with and without base slab.

FEM analysis and test results are shown on Fig. 2 - Fig. 4 of which Fig. 2 shows acceleration response magnification of side wall of the tank model with a base depth of 14cm. Fig. 3 shows a resonance curve of dynamic strain of side wall of the tank model with a base depth of 14cm and Fig. 4 shows the depth directional distribution when in resonance. Further, the first and second natural frequencies of a natural ground model is 6.5Hz and 20Hz respectively.

After analysing all data obtained, the following were clarified;

a. The impact of embedded depth and rigidity of the joint between base slab and wall which appeared on the resonance characteristics of the tank wall is limited within the range of frequency in the neighborhood of the first resonance point of the surrounding soil ground.

b. The existence and non-existence of a base slab affected on the magnitude of dynamic strain of the tank wall section deeper than the central part of the tank and the embedded depth affected particularly normal strain on axial cross sections.

c. With particular reference to ovaling phenomenon, it was found from the analytical result of the three dimensional finite element model that the difference in width between the loading direction and the perpendicular direction of the ground model did not contribute to the generation of ovaling phenomenon. It is therefore anticipated that an error arising from the installation of the tank (i.e. initial imperfection), or an inferior contact of the tank to the ground is responsible for this specific phenomenon.

Further, the above are the results obtained when the tank was empty, but the tests showed no significant difference even when the tank was full.

SEISMIC RESPONSE ANALYSIS OF FULL SIZE INGROUND TANK

Earthquake accelerations in the analysis are simulated as nonstationary amplitude and frequency processes based on the physical spectral model by Hoshiya (Ref.5) for given magnitude M and epicentral distance Δ.

Since this work was already conducted by the Japanese Railway Facilities Association (Ref.6) according to the same analytical technique, we used their results.

Table 2 shows various types of waves employed in this study and Fig. 5 shows its physical spectrum. Also, as a reference, we incorporated into our analytical work El Centro (1940, NS, EL4NS001) and Taft (1952, EW, TFTEW001) accelerations known as severe earthquakes recorded in the past, which were normalized at the maximum acceleration of 150gal. Inground tank and its surrounding soil ground were taken as an axi-symmetric finite element model and response analysis was made through a step-by-step integration procedure by means of the Model Analysis which enabled us to obtain sectional forces, maximum accelerations and displacement of the inground tank and its neighboring soil ground. Fig. 6 shows an outline of soil-tank model.

Also, a total of four models of 60,000kl and 90,000kl tanks each having a base concrete connected by pins (P) or connected rigidly (F) to the tank wall were used.

In this analysis, the variance of transfer function attributable to earthquake accelerations was not taken into account, but stiffness and damping constant taken as average from the response results of free soil obtained on the basis of G/G_0-γ and h-γ curves for each layer were used.

Analytical results are shown on Figs. 7-9 of which Figs. 7 and 8 indicate vertical distribution of normal forces on axial cross section and vertical distribution of bending moment on axial cross section of the tank wall (9-P), and Fig. 9 indicates vertical distribution of maximum sectional forces when Taft acceleration is used. Further, the result of eigenvalue analysis is much the same in any cases. The first, second and third natural frequencies were 0.71Hz, 1.59Hz and 3.23Hz respectively.

As a result of our review on all cases, the following can be said;

a. There were no significant difference noticeable in the eigenvalues of the tank-soil coupling system which will arise from the difference in the embedded depth and rigidity of the joint between base slab and wall.

b. Maximum response displacement of the top part of the tank wall was approximately 50% smaller than that of the soil ground at a distance of 2D away from the tank wall, while maximum response accelerations of the top part of the tank wall remained nearly the same as that of free field. Difference was however noticed on the spectrum shapes of the waves. There was some amplifying trend noticed on the spectrum shape of the part of the tank side wall within the range of 2 - 6Hz.

c. Maximum base acceleration αmax will not be a prime parameter essential to determining whether response is large or small. Should we obtain maximum base acceleration αmax with magnitude M or epicentral distance Δ as parameter and use the past records after normalization, it only serves to meet the requirements of earthquake acceleration αmax and does not help very much for responses. On the other hand, however, phase characteristics of earthquake accelerations largely effect responses.

d. The larger the magnitude M of earthquake acceleration is, the greater all responses will be. Provided that the magnitude M is exactly the same, the longer the epicentral distance Δ is, the larger the displacement and cross sectional forces of the tank will be. This can be explained by the fact that the predominant period of soil ground was relatively a longer period of 1.4sec and, at the same value of magnitude M, the longer the epicentral distance Δ was, the greater the long period components of waves would be.

e. The difference in cross sectional force of the tank wall which generated from the difference in the embedded depth of the tank was not particularly noticeable. The difference in cross sectional force arising from the different rigidity of the joint between base slab and wall was not relatively noticed except that noticeable in part of bending moment of side wall close to a base concrete.

COMPARISON WITH STATICAL ASEISMIC DESIGN METHOD

Figs. 10 and 11 illustrate the results of comparative study with current seismic design method taking as an example a 90,000kl tank with its base concrete connected to the side wall by pins (9-P) which was selected from the results of the foregoing study.

Fig. 10 indicates vertical distribution of normal force on circumferential cross section, while Fig. 11 vertical distribution of bending moment on axial cross section.

Further, the result of calculation of axi-symmetric shell shown on the graph is the envelope plotted of maximum value of 9-P model which was obtained from the analytical result of dynamic response carried out in the previous section.

The design techniques employed for the comparative study were seismic coefficient method and response displacement method. The standard seismic coefficient of the former was set as 0.15 and the latter technique was the method in which the displacement of the ground (6.96cm on the ground surface and 0cm at the bottom of the concrete) was forcibly loaded into the tank by means of springs. Also, static calculation was conducted by FEM analytical method using three dimensional shell elements.

From the above, it can be said that distribution mode of each cross sectional force using response displacement method was approximately the same as the result of dynamic response analyses, while distribution mode of each cross sectional force by seismic coefficient method did not meet the actual requirements. From the view point of seeking the rationality of design, it is necessary that we should study these methods further.

To sum up, it is thought that current design method had sufficiently covered the difference in vibration characteristic arising from the difference in the embedded depth and rigidity of the joint between base slab and wall.

Further, with a view to confirming the reasonableness of a series of such analytical results obtained, we have taken a relatively large acceleration record from the results of the earthquake observation of inground tanks (Ref.1) and checked and reviewed it against the results of our calculations and confirmed that the results of our calculations were nearly the same as the results of the observations.

CONCLUSION

In view of the conclusions of each section, the following final comments are made. The vibration characteristics of inground tanks are considerably governed by vibration characteristics of soil ground. The impact of embedded depth and rigidity of the joint between base slab and wall is clearly noticed in the neighborhood of the first natural frequency point of the surrounding soil ground, but when random waves of earthquake type were loaded, the impact of vibration characteristic of soil ground is large and dynamic response characteristic which are generated from the difference in the embedded depth and rigidity of the joint between base slab and wall will not create any problems regarding design.

REFERENCES

1) M. Hamada, M. Yokoyama and Y. Sugihara; A Study on the Dynamic Stresses of An Underground Tank by Earthquake Observation and Numerical Analysis, 5th Japan Earthquake Engineering Symposium, 1978.

2) Y. Goto and T. Shirasuna; A Seismic Response Characteristics of A Group of Inground Tanks Built in Alluvial Soil Ground, 15th Earthquake Engineering Research Study Meeting, JSCE 1976.

3) E. Saito, et.al.; A Dynamic Behavior of Cylindrical Type Inground Tank (No.5) - Test of its Model Tanks in Group Using Gelatine Gel as a Soil Ground, Proceedings of 34th Annual Academic Lecture Meeting, JSCE 1979

4) H. Nagaoka, et.al.; A Behavioral Analysis of LNG Inground Storage Tanks During Earthquakes, NKK Technical Report No.90, 1981.

5) M. Hoshiya and R. Isoyama; A Simulation on Earthquake Accelerations by Multi-dimentional Non-Stationary Random Processes, Proc. of JSCE, No. 263, Jan., 1978.

6) A Study Report on Aseismic Reinforcement of Railway Civil Structures, Issued by Japan Railway Facilities Association, March, 1981.

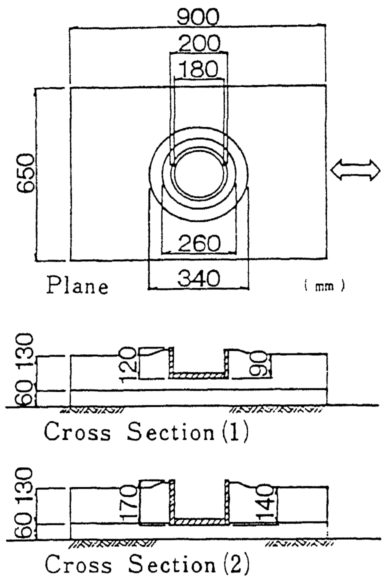

Fig.1 Proto Type Model

Table.1 Physical Constants

		Real	Model
Bottom Layer	Young's Modulus (kg/cm^2)	2400	1.2
	Unit Weight (g/cm^3)	1.8	1.06
	Poisson's Ratio	0.48	0.48
	Damping Ratio	0.3	0.3
Top Layer	Young's Modulus (kg/cm^2)	940	0.47
	Unit Weight (g/cm^3)	1.8	1.06
	Poisson's Ratio	0.48	0.48
	Damping Ratio	0.3	0.3
Tank Wall	Young's Modulus (kg/cm^2)	2.48×10^5	124
	Unit Weight (g/cm^3)	2.5	1.47
	Poisson's Ratio	0.48	0.48
	Damping Ratio	0.3	0.3

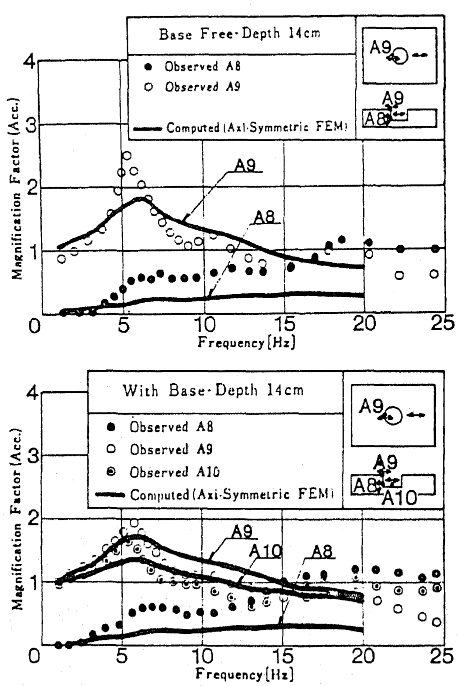

Fig.2 Resonance Curve(Acc.)

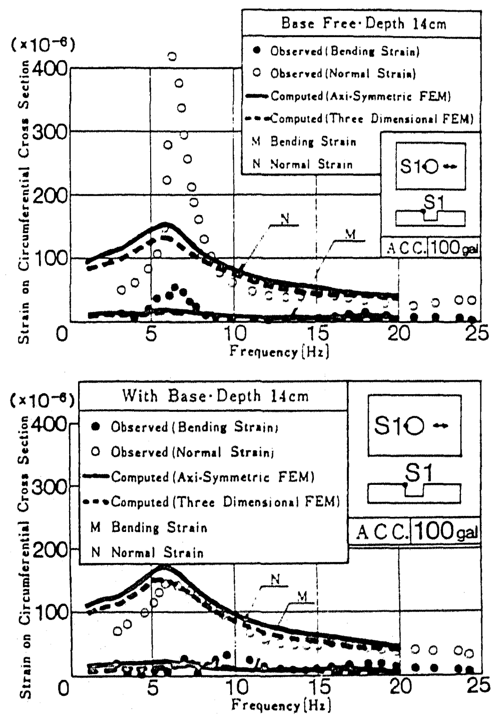

Fig.3 Resonance Curve(Strain)

Table.2 Earthquake Accelerations

No.	Acceleration	Magnitude M	Epicentral Distance Δ (km)	Max. Acc.	Duration (sec)
1	S1.1.(1)	M<5.5	0≦Δ<40	127	20
2	S3.1.(1)	6.5≦M<7.5	0≦Δ<40	210	20
3	S3.1.(2)	6.5≦M<7.5	0≦Δ<40	312	20
4	S3.3.(1)	6.5≦M<7.5	80≦Δ<160	129	20
5	S3.3.(2)	6.5≦M<7.5	80≦Δ<160	174	20
6	EL4NS001	–	–	150	20
7	TFTEW001	–	–	150	20

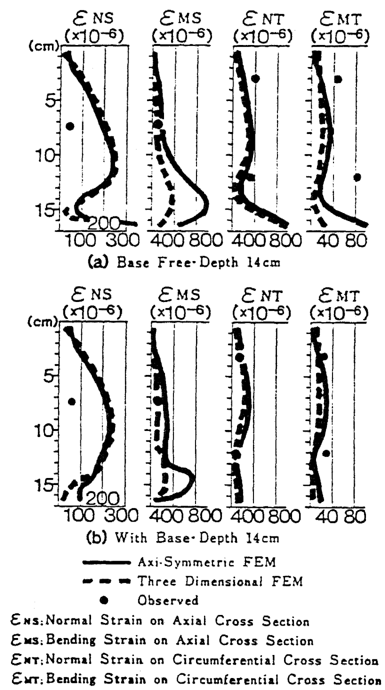

Fig.4 Vertical Distribution of Strain

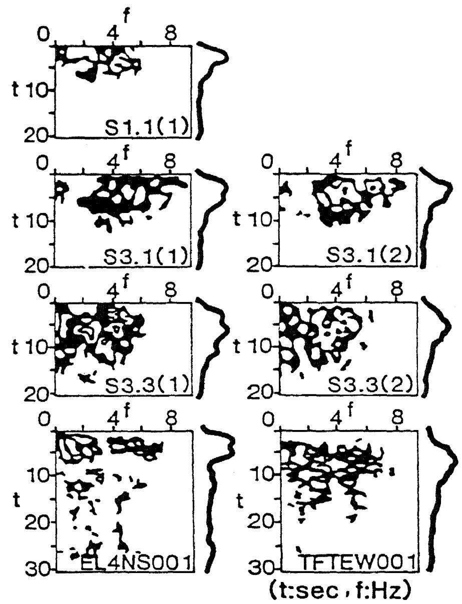

Fig.5 Physical Spectrum

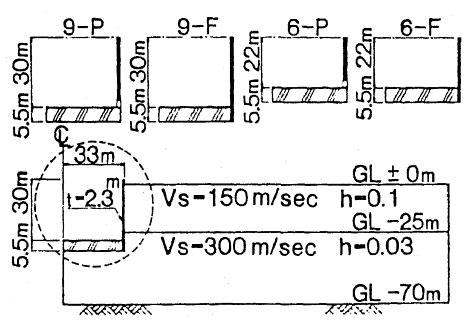

Fig.6 Model of Inground Tank

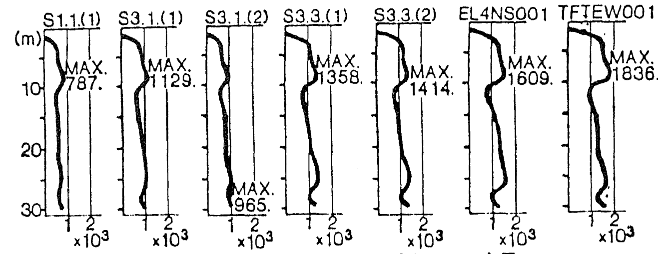

Fig.7 Vertical Distribution of Normal Force on Axial Cross Section[Ns(kg/cm)·9-P]

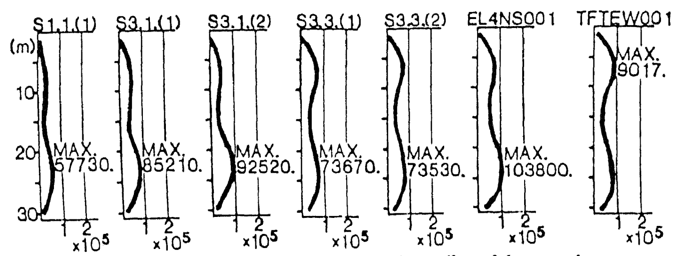

Fig.8 Vertical Distribution of Bending Moment on Axial Cross Section[Ms(kg·cm/cm)·9-P]

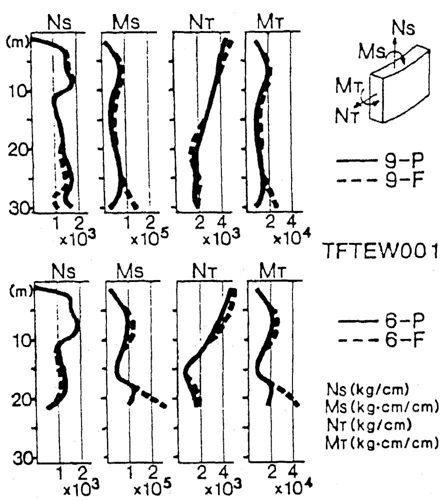

Fig.9 Vertical Distribution of Sectional Forces

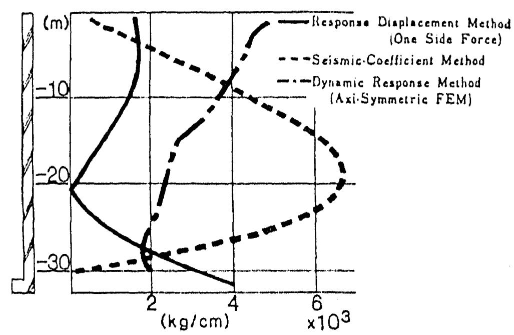

Fig.10 Vertical Distribution of Normal Force on Circumferential Cross Section(Nt)

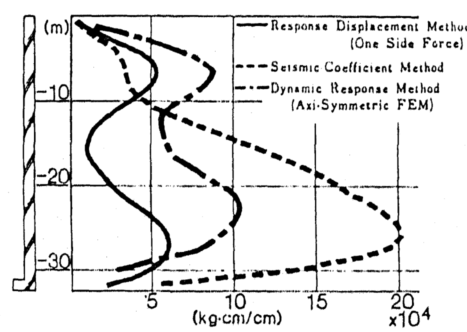

Fig.11 Vertical Distribution of Bending Moment on Axial Cross Section(Ms)